Brownian Motion in a Non-Newtonian Fluid

by

James W. Kennington

THESIS

Presented to the Faculty of the Department of Physics of
The University of Texas at Austin
in Partial Fulfillment
of the Requirements
for the Degree of

BACHELOR OF SCIENCE

PHYSICS, DEPARTMENTAL HONORS

THE UNIVERSITY OF TEXAS AT AUSTIN
May 2015

Acknowledgments

The list of names I wish to thank for supporting me through to this point could fill another thesis, so I will simply say that I dedicate this effort to my family, to Vignesh, and to all those who have kept me going through good times and bad.

I owe especial gratitude to Jianyong Mo, David Riegler, Akarsh Simha and Dr. Mark Raizen for their continued mentorship and patience. I could not have completed this without each of you.

Brownian Motion in a Non-Newtonian Fluid

James W. Kennington
The University of Texas at Austin, 2015

Supervisor: Dr. Mark Raizen

I examine the theoretical framework required to analyze the motion of a Brownian particle in a non-Newtonian fluid for purposes of rheological classification. The tools of continuum mechanics are presented as means to constructing continuous models for fluid dynamics, and the Maxwell and Kelvin-Voigt fluid models are then constructed accordingly. Brownian motion is introduced and the relation to the Wiener Process and Einstein formulations are considered. Ultimately, I derive a relation between the frequency-dependent dynamic viscosity and the autocorrelation of the Brownian velocity. This relation is useful in optical microrheological contexts as it enables the microscopic determination of fluid properties which may be used to identify fluid classes. I then present the computational framework required to process experimental data and minimize the associated, non-trivial numerical error.

Table of Contents

Chapter 1

Introduction

1.1 Rheology

Deriving its name from the greek word for flow, the field of Rheology is primarily concerned with modeling and measuring the deformation and flow of matter [12]. Since the early 1920's, physicists and chemists have sought a better understanding of the internal response to external forces in a variety of materials. It is largely held that Dr. Eugene Bingham founded the field of study while pioneering concepts of fluidity and deformation response, coining the name of the discipline with the help of colleague Dr. Markus Reiner [5]. Bingham also went on to successfully model new types of fluid behavior, such as plasticity, and some still bear his name to this day. The so-called "Bingham plastic" was surprisingly poorly understood given the relative banality of the most common examples, such as mayonnaise; however, Bingham was able to successfully unite the low-stress, rigid behavior and high-stress fluid behavior under a single mathematical framework [4].

Since Bingham's initial trailblazing work, the field of Rheology has vastly expanded. Tasked with accurately characterizing material deformation, modern researchers seek to associate external forces and pressures with internal responses. Of particular interest are materials with non-ideal blends of

fluid and solid behavior. While a variety of techniques, both analytical and empirical, are employed to probe these relations, the continuum approach has risen to the top of competing frameworks due to its simplifying assumptions and relatively-improved ease of manipulation. Since it is known that materials are composed of smaller units, such as molecules, atoms, or particles, intuition would suggest a hierarchical model of material deformation; however, handling the vast number of units proved challenging, even with the tools of statistical mechanics. A comparatively simple solution was to treat the materials as continuous matter, which offered reduced mathematical complexity but also introduced new *rheological parameters* to describe the continuous models. These new parameters were mostly intended to be found empirically, alongside other physical quantities of interest in rheology, such as elasticity, viscosity, viscoelasticity, and plasticity.

The persistent connection between rheology and empirical measurement is no accident; the field has always had close ties to material science and chemistry, due to the considerable overlap in subject matter. In the study of polymers, rheology seeks to understand the elastic and potentially viscous behavior of rubbers, plastics, and fiber mixtures. Such knowledge of polymers is highly useful for everyday applications such as car tire design, but may also be used to model more complicated phenomena such as material damage and fracturing. In the concrete engineering industry, workability and utility are dependent upon rheological properties of cement paste, which is considered to be a semi-fluid. The ability to use concrete in practice depends upon how

the paste may be applied, how long it takes to solidify, and how it responds to environmental conditions. These key characteristics may be modeled using the continuum framework of modern rheology. Another example of interest pertains to the medical manipulation of bodily fluids. Hemorheology, in particular, studies properties of blood and blood elements, which is essential to the development of biotechnology dealing with blood transfusions, and cleaning. These examples only serve to highlight the development and relevance of modern rheology, as well as emphasize the future need thereof.

1.2 Microrheology

Where the field of rheology initially intended to describe macroscopic phenomena occurring due to the deformation of materials, several other approaches and applications of rheology have since gained considerable momentum. Empirical rheology, true to its name, is primarily concerned with the experimental determination of constants and functions that characterize observed phenomena. Applied rheology, also appropriately named, emphasizes the practical application of observed phenomena and the empirically determined relationships to everyday challenges. Lastly, but most relevant to this paper, microrheology attempts to explain rheological phenomena on a molecular or particle scale [9].

Seeking to connect microscopic structure of a material to its rheological properties, the field of microrheology aims to answer questions of solid-fluid like behavior from the inside out, as opposed to the outside in. The altered

perspective on rheology has technical advantages as well. Microrheological techniques allow for a wide frequency range of observation, from around 10^3 Hz by full-frame multi particle tracking to around 10^6 Hz from photodiode position detection [7]. The use of a local probe to detect properties of a material from the inside of the material gives a more detailed, useful description of the material in terms of model construction. These localized insights are crucial to developing and testing specific rheological models, especially in instances where bulk methods give average distributions that are nearly impossible to decompose into base elements. Microrheological techniques are also more sensitive measures of viscosity and elasticity. A tested sample with low viscous or elastic properties, such as water, have no distinguishable traits by macro methods, such as rheometers; however, microrheological probes are ideally suited to such an environment, and provide excellent signal-to-noise. Perhaps a more tangible, relative benefit of microrheology is that testing procedures require much less of the tested material, which is important both from a conservation perspective, but also from a cost perspective. Also, the equipment is usually less expensive. For instance, a modern rheometer can cost around $100,000, whereas particle tracking equipment can be bought or built for much cheaper [9].

For all of its benefits, microrheology does have noteworthy limitations. Microrheology is largely limited to transparent or spatially-transparent materials, since particle tracking methods require the ability to see the particle visually. Some variants of microrheology, such as magnetic microrheology, are

less dependent upon direct optical view of the tagged particle than other variants, such as optical microrheology [19]. Also, microrheological techniques can be challenging to perform on very elastic or very viscous materials, due to the limited frequency domain of observation as well as the limited possible applied force on the tracked particle. The largest challenge with microrheological techniques; however, comes after observation. The analysis required to make sense of microrheological data is often a few orders of magnitude more time consuming than the actual experimental observation [9]. Analytical methods represents an area of non-trivial concern, and will be addressed towards the end of this paper.

1.3 Optical Microrheology

A sub discipline of microrheology, optical microrheology relies heavily upon the use of optical instruments, such as light scattering detection or high-powered lasers, in order to track the motion of tracer particles in a semi-transparent fluid. Fundamentally, optical techniques in microrheology aim to *see* particles move in a given fluid; however, there are several different methods for by which particles may be successfully tracked. Some ambitious techniques attempt to capture data in a nearly-human way, in that the acquisition process mimics more or less the process that occurs in the human brain when watching the particle move. More specifically, image velocimetry, a popular choice for two-dimensional experiments, relies on image analysis and blob-detection algorithms to locate tracer particles in successive images. The reduction of

image data eventually produces the path of the tracked particle as observed visually. These techniques are non-trivially limited by the frame rate and focal length of the camera. Other techniques are less similar to the human process of observation; they do not involve image analysis, but rather convert an analog signal proportional to the particle's displacement and convert it into a time series of position values. These methods require no images to be taken, nor processed, and are often easier to construct [11].

In addition to different tracking methods, there are two fundamentally different types of particle manipulation. Passive methods aim to track a particle that is entirely free to move about the fluid, whereas active techniques manipulate the position of the particle at some scale. The immediate benefit to the active tracking methodology is that the tracer particle is comparatively easier to follow since it may be confined to a relative region of the fluid.

Among active microrheological techniques, the optical tweezer, or the use of a highly focused laser beam to create a potential well, has gained wide appreciation for its relative ease of manipulation as well as reliable particle tracking. Optical tweezers are also appealing from a theoretical perspective, as the mechanism of confinement is well approximated by a simple restorative force. The physics of optical tweezers will be discussed in greater detail further on in this paper.

Chapter 2

Continuum Mechanics

Composed of molecules, atoms, and particles, matter is known not to be continuous. However, attempting to account for each individual unit of a material is mathematically rigorous if not impossible. Approximate methods, such as statistical mechanics, become necessary for even the smallest, non-trivial, microrheological model sizes, and are yet limited to numerical results in most cases [22]. In order to obtain more wieldy, analytical models, it is necessary to treat the material as a continuum. The simplicity gained by employ of continuous-matter treatment is apparent in situations such as water flow in a pipe, which would be unthinkably challenging to handle with a discretized treatment. Attempting to model all interactions between fluid elements would inevitably require statistical simplifications, which would result in limited solutions. As opposed to dealing with large systems of constituent equations, continuum mechanics uses constitutive equations, which describe the entire material. In order to make such descriptions, continuum mechanics assumes that each material unit is physically identical to any other. This means that any interchange operations would have no effect, unlike in particle based models, where particles may be distinguishable [3]. For instance, the water near the wall of the pipe is not physically different from the water near

the center of the pipe, and if they were to be exchanged, no difference in behavior would be detectable. Continuum mechanics also uses different physical quantities to describe physical phenomena than classical mechanics, such as stress, strain, and a variety of behaviorally-classified responses as opposed to forces, torques, and accelerations. It is clear, then, that a proper review of continuum mechanics is essential to further discussion of fluids in general, but especially for non-newtonian fluids.

2.1 Stress

In the context of continua, stress represents the internal distribution of forces per area in a material. In other words, stress is a way of describing the vectors of force and area at *each point* inside a material. However, before discussion of stresses can take specific form, a context must be established for the material. It is common to let the term *body* refer to the material and *environment* refer to all things that are not the body of interest. The orientation of the body may be described by a simple, right-handed Euclidean basis $\mathbf{E} = \{e_1,\ e_2,\ e_3\}$, where $e_1 \times e_2 = e_3$. In this framework, both force and area are 3-vectors, where area may be described by the corresponding normal vector $\hat{n}$. Therefore, it is sensible that there are a total of 9 degrees of freedom involved in any mutually complete representation [15]. To account for all degrees of freedom, stress most commonly takes the mathematical form of a tensor, typically in the representation put forth by Cauchy, who justified this representation by proving that the state of stress at a given point in the

body is completely described by all possible stress vectors associated with all planes passing through the point [9]. The general form of the Cauchy stress tensor may be simplified to account for the symmetry of stress, reducing the number of independent degrees of freedom to 6.

$$\boldsymbol{T} = \begin{bmatrix} T_{11} & T_{12} & T_{13} \\ T_{21} & T_{22} & T_{23} \\ T_{31} & T_{32} & T_{33} \end{bmatrix} = \begin{bmatrix} T_1 & T_{12} & T_{13} \\ T_{21} & T_2 & T_{23} \\ T_{31} & T_{32} & T_3 \end{bmatrix} \tag{2.1}$$

In most contexts, however, the stress *vector* is of more concern than the entire tensor, since stress is more intuitively described with a reference surface. If the surface may be represented by the normal vector $\hat{n}$, then the corresponding stress vector $\boldsymbol{\sigma}^{(n)}$ may be defined with respect to the surface.

$$\boldsymbol{\sigma}^{(n)} = \hat{n} \cdot \mathbf{T} \tag{2.2}$$

With a proper contextualization of stress, it is easier to define some of the more relevant stress vectors of interest in rheological experiments. The *normal* stress σ_ν is defined as the magnitude of the stress components parallel to the normal vector of the surface, and may be given in terms of the stress vector and surface normal. As expected, the *shear* stress σ is defined as the magnitude of the stress components that are perpendicular to the surface normal, and may be defined in terms of the total stress vector and the normal stress vector in a conventional Pythagorean way.

$$\sigma_\nu = \boldsymbol{\sigma}^{(\boldsymbol{n})} \cdot \hat{n} \tag{2.3}$$

$$\sigma = \sqrt{\left(\boldsymbol{\sigma}^{(\boldsymbol{n})}\right)^2 - \sigma_\nu^2} \tag{2.4}$$

2.2 Strain

In terms of continuous media, strain may be thought of as a measure of a body's response to external forces. Specifically, strain measures a body's deformation under known external forces, and is a way to relate the internal stresses of a body with its deformation. The strain tensor $\boldsymbol{\gamma}$ may be defined in terms of the displacement gradient tensor $\nabla \mathbf{u}$ and its transpose $\nabla \mathbf{u}^T$ by removing the rotational aspects of the displacement vector and using only linear displacements [15]. The stress vector $\boldsymbol{\gamma}^{(n)}$ may be defined in terms of the strain tensor and a reference surface normal $\hat{n}$.

$$\boldsymbol{\gamma} = \frac{1}{2}\left(\nabla \mathbf{u} + \nabla \mathbf{u}^T + \nabla \mathbf{u}^T \nabla \mathbf{u}\right) \tag{2.5}$$

$$\boldsymbol{\gamma}^{(n)} = \hat{n} \cdot \boldsymbol{\gamma} \tag{2.6}$$

Similar to stress, there are some relevant strain vectors that are of particular interest in rheology. The *normal* strain γ_ν is defined as the magnitude of the strain components parallel to the surface normal, and the *shear* strain γ is defined as the magnitude of the strain components perpendicular to the surface normal, or parallel to the surface.

$$\gamma_\nu = \boldsymbol{\gamma}^{(n)} \cdot \hat{n} \tag{2.7}$$

$$\gamma = \sqrt{\left(\boldsymbol{\gamma}^{(\boldsymbol{n})}\right)^2 - \gamma_\nu^2} \tag{2.8}$$

In the context of deformations, is it useful to think of the shear strain as taking place *in the plane* of the surface of interest. In many cases, the normal strain is negligible and the shear strain is of primary concern.

2.3 Elastic Response

In an ideal elastic solid, no matter what torturous forces and torques are applied to the body, it will always reassume its original shape. In other words, it will behave purely *elastically*. This example highlights the essence of the elastic response, in that the material manages to perfectly preserve the initial state of the body. The ability of the material to compensate for all displacements suggests the existence of a material *memory*, and in the case of the pure elastic response, perfect memory. The physical mechanism behind the elastic memory of continuous materials is somewhat analogous to a similar memory possessed by springs. A ideal spring will always return to equilibrium when all applied forces are removed, and is defined as possessing linear, limitless elasticity. Energy transferred to the body by the applied forces is *stored without loss* as potential energy in the spring. Similarly, perfectly elastic materials store the energy of the external forces that cause deformations, which allows the body to return to equilibrium once the external forces have been removed. The well-known Hooke's Law supplies the necessary tools for dealing with linear elasticity, and Hooke's Law for solids is a recasting of the original principle in terms of stress and strain.

$$\sigma = G\gamma \tag{2.9}$$

Though it is simple, Hooke's law for solids powerfully relates the stress σ and strain γ in terms of a linear response coefficient G, called the *elastic modulus*. The elastic modulus is an important rheological parameter, and will be discussed in greater detail in a dynamic context.

2.4 Viscous Response

Contrary to the behavior of an ideal elastic solid, an ideal viscous fluid will permanently retain all deformations after external forces abate. In terms of memory, the ideal viscous response is pure amnesia; the body has absolutely *no memory* of its initial state before external forces were applied, and consequently cannot attempt to regain its previous form. Since the viscous response offers no resistance to displacement, definition of the response must involve the rate of displacement, more specifically, the *strain rate* $\dot{\gamma}$. Newton's law for fluids defines the relationship between stress and (shear) strain rate for the linear viscous response.

$$\sigma = \eta\dot{\gamma} \tag{2.10}$$

Despite the simple appearance, Newton's law for fluids succinctly relates the stress σ and shear rate $\dot{\gamma}$ by means of a linear response coefficient η, called the *dynamic (shear) viscosity*. Much like the elastic modulus, the dynamic viscosity is a significant rheological parameter, and is often the objective of experimental measurements. As described above, the viscosity is constant; however, this is often not the case. In such cases, the dependencies of the dynamic viscosity are critical to characterizing the appropriate rheological model for the fluid. The dashpot is widely held as a classical analog of the viscous response, in that the applied energy is dissipated as the piston moves through the fluid of the dashpot, and the result is an acceptance of displacement.

2.5 Viscoelastic Response

As the name would suggest, the viscoelastic response is an instantaneous combination of elastic and viscous responses. Most materials are viscoelastic, with different timescales on which the elastic and viscous responses dominate. However, the fact that the two responses have different timescales of dominance should not suggest an order of response. In fact, both responses are continually responding to external forces, and the combination of the two responses characterizes the viscoelastic material. In order to characterize this complex behavior, the *dynamic modulus* is measured. In complex representation, the dynamic modulus describes the overall response of a viscoelastic material to *oscillatory* external forces by relating the elastic modulus of the material to the strain rate, which is similar to the viscosity parameter. However, the exact relation depends upon the construction of the model, several of which will be discussed below. In general, the complex dynamic modulus may be composed of a storage and loss component, corresponding to elastic and viscous responses respectively [9].

$$G^* = G' + iG'' \tag{2.11}$$

$$G' = \kappa \cos(\phi) \tag{2.12}$$

$$G'' = \kappa \sin(\phi) \tag{2.13}$$

Where G' represents the storage component and G'' represents the loss component, both of which are related by a phase angle ϕ. The constant κ is a material parameter relating the magnitudes of stress and strain. In the case

of the pure elastic response, the stress and strain are perfectly in phase $\phi = 0$, but in the case of pure viscosity, stress leads strain by a phase angle of $\pi/2$ radians. Understanding the response of a viscoelastic material in terms of an oscillatory stress has innumerable applications, since most very few forces in nature are truly static. For instance, consider the rubber soles of a person standing still. While the applied stress may appear macroscopically constant, the person is actually shifting their weight ever so mildly, but largely enough to cause microscopic oscillations. Microrheology probes the dynamic moduli of materials to understand such complex problems as tearing and microfracturing of rubber under oscillatory strains. Therefore the dynamic modulus is of great importance to understanding materials at the microscopic level.

Chapter 3

Fluid Models

3.1 Simple Fluids

A simple fluid is defined to be a fluid that exhibits only a single type of behavior. In the case of a simple viscous fluid, which is by far the most relevant to real fluid models, the fluid has a linear response to stress. Called *Newtonian* fluids, the viscous response follows Newton's law for fluids, a simple linear relationship between stress and strain rate given by Equation 2.10. More rigorously, a fluid is considered to be Newtonian if the stress tensor is constant. If the stresses throughout the fluid may be considered isotropic, then the stress tensor is diagonalizable under the transformation $\mathbb{T} : \mathbf{E} \rightarrow \mathbf{E}'$, where $\mathbf{E}' = \{\hat{n}, e_2', e_3'\}$ is defined in terms of the surface normal. This means that the viscosity can be completely reduced two terms, the shear and normal viscosities, since only 1 of the 3 principal viscosities will be normal and the other two will be in the plane of the surface. Under the assumption of incompressibility, the normal stresses may be neglected. Therefore, the shear viscosity is the sole parameter of interest for Newtonian fluids.

3.2 Complex Fluids

Much more often in nature, a fluid will posses more than a single type of stress response. A fluid is deemed complex if it exhibits multiple types of behaviors. While this definition is largely vague, most complex fluids can be regarded as twofold; a complex fluid usually exhibits two types of behaviors, such as a solid-liquid mixture, or liquid-gas mixture [9]. Modeling the dynamics of flow in complex fluids is convoluted due to the coexistence of multiple matter phases, and nonlinear effects may arise from the interaction between matter phases. In optical microrheology, microparticles are used to track flows in complex fluids to better understand the microfluidics created by the interaction of multiple matter phases [10]. This paper will restrict scope to Non-Newtonian fluids, which are a special type of complex fluid resulting from a mixture of liquid and solid behaviors.

3.2.1 Non-Newtonian Fluids

As mentioned above, non-Newtonian fluids are a type of complex fluid; however, the negative definition states that all fluids that do not exhibit strict linear dependence between stress and shear rate are non-Newtonian. In most cases, the viscosity is not static, but rather is dynamic and dependent upon shear rate. The dependence of the viscosity upon the shear rate or shear frequency is the most fundamental, measurable quantity of a complex fluid, and is what helps categorize different types of non-Newtonian fluids. Fluids

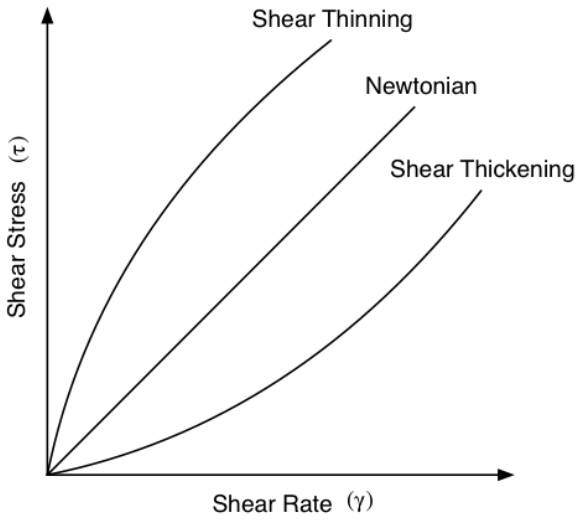

Figure 3.1: Non-Newtonian viscosity behaviors.

whose viscosity decreases with shear rate, such as whipped cream or silicone oil, are called *shear-thinning*, whereas those whose viscosity increases with shear rate, such as corn starch and water mixtures, are called *shear-thickening*.

3.3 The Maxwell Model

Simplest of all fluid models, the Maxwell model describes a fluid as the linear combination of an elastic element and a viscous element in series. Fluid models are often represented as classical circuits, in which strain behaves as voltage and stress behaves like current. As shown in Figure 3.2, the Maxwell

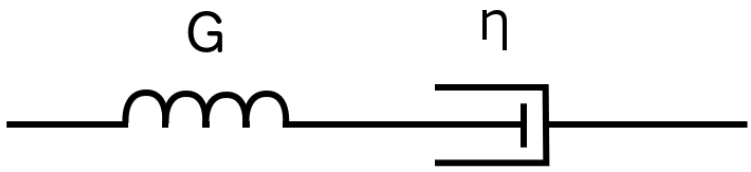

Figure 3.2: Maxwell model diagram.

model consists of a spring element and dashpot element in series. Like a circuit, in which the current passing through the loop is the same for all elements, the stress is the same for both elements of a Maxwell fluid. Similarly, the strain behaves like circuit loop voltage, in which the total system strain is additive across the elements of the loop.

$$\begin{aligned} \sigma &= \sigma_e = \sigma_v \\ \gamma &= \gamma_e + \gamma_v \end{aligned} \tag{3.1}$$

When a strain is applied to a Maxwell fluid, the spring initially absorbs the imparted energy, but as time increases, the energy is transferred to the dashpot and dissipated. Therefore, the fluid will behave elastically on short timescales and viscously on long timescales. The threshold where these timescales meet is

called the *relaxation time*, or the Maxwell time, and is denoted τ_m. The elastic stress σ_e and the viscous stress σ_v may be used to determine the characteristic, or Maxwell time. As depicted in Figure 3.3, the Maxwell time may be found by equating and elastic stress response σ_e and a viscous stress response σ_v. Using the relation for elastic stress given in Equation 2.9 and the relation for

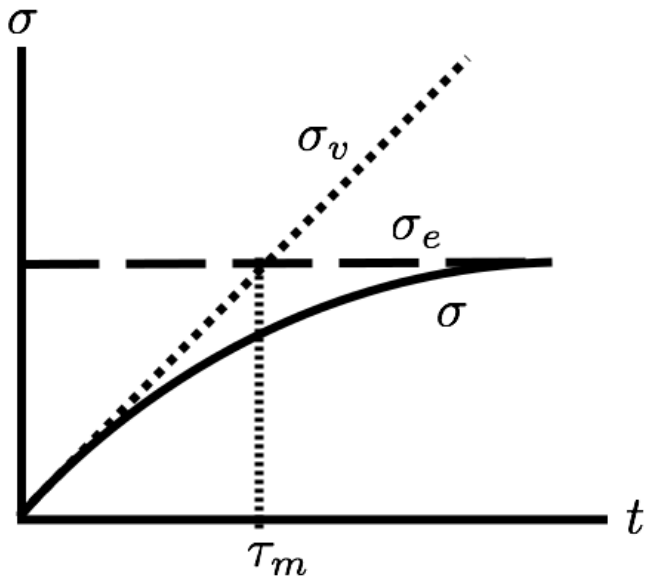

Figure 3.3: Maxwell model element stresses.

viscous stress given in 2.10, the Maxwell relaxation time τ_m may be found by solving for the configuration where the two fluid elements have equal stress responses, $\sigma_e = \sigma_v$. The result may then be used to determine the overall constitutive equation for the Maxwell model that relates stress and strain.

$$\eta\dot{\gamma} = \sigma_v = \sigma_e = G\gamma = G\dot{\gamma}t \quad \rightarrow \quad \tau_m = \frac{\eta}{G} \tag{3.2}$$

$$\tau_m\dot{\sigma} + \sigma = \eta\dot{\gamma} \tag{3.3}$$

Where the elastic stress has been expanded $\gamma = \dot{\gamma}t$. In the case where the two responses overlap, the time becomes the Maxwell relaxation time, $t = \tau_m$. Equation 3.3 is also referred to as the Maxwell equation, and shows that the stress is dependent both upon the shear and the shear rate.

3.4 The Kelvin-Voigt Model

As in the Maxwell Model, the kelvin model also bears a useful circuit analog. Of similar simplicity, the Kelvin-Voigt model is composed of a linear combination of an elastic element and a viscous element in parallel. Like a

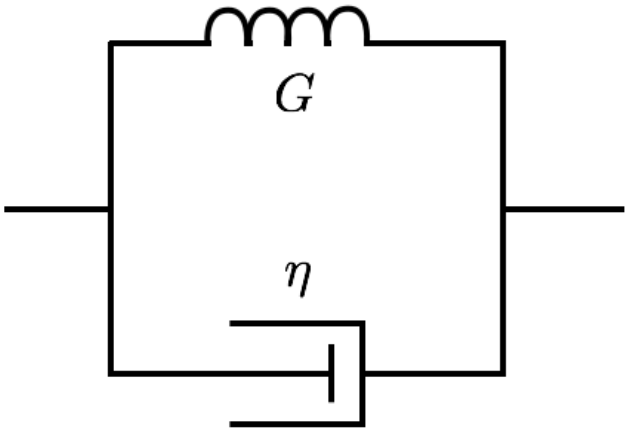

Figure 3.4: Kelvin-Voigt model diagram.

circuit, in which voltage is the same across multiple circuit branches, the strain is the same for both fluid elements. continuing with the circuit analogy, the total stress applied to the system behaves like current, in that it is divided among branches. Therefore, the total stress of the fluid is additive over both fluid elements.

$$\begin{aligned} \sigma &= \sigma_e + \sigma_v \\ \gamma &= \gamma_e = \gamma_v \end{aligned} \tag{3.4}$$

When strain is applied to a Kelvin-Voigt material, the two responses are immediately apparent; however, depending upon the fluid model parameters, one behavior may modulate the other. For instance, if the material has a strong viscous response but a relatively weak elastic response, then the elastic response will modulate the long time behavior of the viscous response. On shorter timescales, the modulation is reversed [9]. Using the relation for elastic stress given in Equation 2.9 and the relation for viscous stress given in 2.10, the Kelvin-Voigt material may be described by a single identifying parameter τ_{kv}, the Kelvin-Voigt characteristic time.

$$\frac{\sigma}{G} = \gamma_e = \gamma_v = \frac{\sigma}{\eta}t \quad \rightarrow \quad \tau_{kv} = \frac{\eta}{G} \tag{3.5}$$

$$\tau_{kv} = \frac{\eta}{G} \tag{3.6}$$

The constitutive equation for the Kelvin-Voigt Model may be found by application of 3.6 to 3.4, and by using the Hooke and Newton relations for the elastic and viscous components, respectively.

$$\sigma = G\gamma + \eta\dot{\gamma} \tag{3.7}$$

$$\gamma(t) = \frac{\sigma_0}{G}\left(1 - e^{-t/\tau_{kv}}\right) \tag{3.8}$$

Chapter 4

Brownian Motion

When botanist Robert Brown first observed small grains of pollen moving about in water in 1827, the motion of the pollen particles seemed to defy ordinary explanation. The paths travelled by individual particles seemed to be random, but not perfectly so. This motion, deemed Brownian motion after its first observer, would take nearly another century to be quantified mathematically, and slightly longer to be explained physically [20].

4.1 Einstein Formulation

Suspecting that the motion of the pollen particles was due to collisions with individual water molecules, Einstein began to unravel the mystery in terms of particle densities of the fluid. By modeling the fluid as a collection of water molecules and using results of statistical mechanics, Einstein was able to formulate the problem of brownian motion as one of diffusion with respect to the particle density ρ.

$$\frac{\partial \rho}{\partial t} = D\frac{\partial^2 \rho}{\partial x^2} \tag{4.1}$$

$$\rho(x,t) = \frac{N}{\sqrt{4\pi D t}} e^{\frac{x^2}{4Dt}} \tag{4.2}$$

The solution to 4.1 allowed for the calculation of moments, which ultimately led to the mathematical classification of Brownian motion. The first few statistical moments help characterize Brownian motion. If a family of Brownian trajectories $\{x(t)\}_{t\geq 0}$ is observed, then 4.3 shows that the average position is zero; in other words, the first moment shows that Brownian motion is unbiased in terms of direction. The second moment of the difference may also be taken, and 4.4 shows how the mean square displacement (hereafter MSD) may grow linearly with time.

$$\overline{x(t)} = 0 \tag{4.3}$$

$$\overline{(x(t) - x(t'))^2} = 2D|t - t'| \tag{4.4}$$

$$\overline{(x(t) - x(0))^2} = 2Dt \tag{4.5}$$

However, Einstein's formulation of Brownian motion also makes some unphysical predictions. Since the notion of Brownian motion is the extension of a random walk to an infinitely small step size and infinitely small time interval, the instantaneous velocity may be defined accordingly.

$$v(t) = \lim_{\Delta t \to 0} \frac{x(t) - x(t')}{\Delta t} = \lim_{t \to t'} \frac{\sqrt{(x(t) - x(t'))^2}}{t - t'} \tag{4.6}$$

$$\overline{v(t)} = \lim_{t \to t'} \frac{\sqrt{\overline{(x(t) - x(t'))^2}}}{t - t'} = \lim_{t \to t'} \frac{\sqrt{2D|t - t'|}}{t - t'} = \lim_{t \to t'} \sqrt{\frac{2D}{t - t'}} = \infty \tag{4.7}$$

Therefore, the fractal nature of the Einstein formulation of Brownian motion, which will be further examined as a Wiener process, implies that the instantaneous process of a Brownian particle is infinite, or physically immeasurable. However, it has been shown experimentally that the instantaneous

velocity of a Brownian particle is, in fact, measurable [18]. Therefore, it must be concluded that, while mathematically elegant, the Einstein formulation of Brownian motion is incomplete. In order to fully understand the motion of a Brownian particle, the understanding of the environment must be corrected. The assumptions of statistical mechanics ignore hydrodynamic effects, but these must be included in relation to the motion of the particle, as will be demonstrated below in discussion of the Langevin Equation.

4.2 The Wiener Process

The mathematical formulation of Brownian motion deserves special attention, due to its significance to the study of random processes. The Wiener process is considered to be the *standard* Brownian motion, defined formally as a stochastic process with several important characteristics. First, the Wiener process is continuous, such that the family of random variables $\{x(t)\}$ have zero first moment $\overline{x(t)} = 0$. Second, the Wiener process is also defined to have autocorrelation function proportional to the diffusion constant and time difference.

$$\langle x(t)x(t')\rangle = 2D\min(t,t') \tag{4.8}$$

The Wiener process is also considered to be the *stochastic integral* of a white noise. This relates directly to the study of Brownian motion in fluids since the thermal forces inside a fluid are often modeled with white noise. For further elaboration on the autocorrelation function or white noise, see Appendices A.1 and A.2, respectively.

4.3 Ergodic Hypothesis

The Ergodic hypothesis fundamentally asserts that in certain statistical contexts, the average properties of a dynamical system over time and the average statistical ensemble properties are identical. This is significant since it suggests that two parts of the same process $x(t)$ over two intervals $I_1 = [t_1, t_1']$ and $I_2 = [t_2, t_2']$ are essentially distinct stochastic processes, provided that the intervals I_1 and I_2 are far enough apart to exceed the memory of the environment. This means that long timescale observations of Brownian motion, which is a dynamical system, may be split into smaller time intervals, each of which may be considered to be causally independent. Therefore, each smaller interval may be treated as a separate system. The implications of the ergodic hypothesis are of paramount importance to experiments in microrheology that use the Brownian motion of tracked particles to detect properties of fluids, because it saves the lab time and resources, in that we may build only one apparatus, yet claim the statistical advantages of having built thousands of apparati. Though seemingly trivial, this important theorem enables the data analysis to be performed, and allows the usage of well known statistical results of Brownian motion, such as the moments and autocorrelation function.

Chapter 5

Frequency Dependent Dynamic Viscosity

The frequency dependent dynamic viscosity is a parameter of rheological significance, since it may be used to help identify fluid models. This parameter may be directly related to the time series of a Brownian motion, and is therefore a measurable quantity. The ability to measure the FDDV implies that experimental determination of fluid type is possible, and merits explanation. The necessary results will be derived, and applications will be demonstrated later on.

5.1 Derivation

Before beginning the derivation, it is necessary to define the dynamic viscosity, and to note how it differs from the conventional viscosity. From Newton's law for fluids, Equation 2.10, the dynamic viscosity is defined in terms of the linear response of stress to strain $\sigma = \eta\dot{\gamma}$. The frequency dependent dynamic viscosity (hereafter FDDV) is simply a non-constant functional form of the newtonian viscosity.

$$\sigma = \eta(\omega)\dot{\gamma} \tag{5.1}$$

Let $C(t)$ represent the velocity autocorrelation function (VACF), which measures the memory of the velocity of the Brownian motion $x(t)$. Let $\hat{C}(\omega)$ represent the positive-time Fourier transform of the VACF.

$$C(t) = \langle v(t)v(0)\rangle \tag{5.2}$$

$$\hat{C}(\omega) = \int_0^\infty C(t)e^{-i\omega t}dt \tag{5.3}$$

The admittance of the fluid is defined as the linear response of the Fourier transform of the velocity of the Brownian particle to an oscillatory driving force.

$$\hat{v}(\omega) = \mathcal{Y}(\omega)\hat{E}(\omega) \tag{5.4}$$

Where $\mathcal{Y}(\omega)$ represents the admittance of the fluid, $\hat{v}(\omega)$ the Fourier-transform of the particle velocity, and $\hat{E}(\omega)$ the oscillatory driving force.

From the Fluctuation-Dissipation theorem, the admittance and VACF may be related directly [8].

$$\hat{C}(\omega) = k_B T\ \mathcal{Y}(\omega) \tag{5.5}$$

Where k_B is the Boltzman constant, and T the temperature. This relation motivates the derivation of the admittance, which may be done by beginning with the general Langevin equation. The general Langevin equation relates the forces acting within a fluid.

$$m\dot{v} + \zeta \star v + k\int vdt = E(t) \tag{5.6}$$

Where m is the mass of the particle, ζ is the viscous friction within the fluid, and k is the harmonic potential constant generated by the optical tweezer. Taking the Fourier transform of the general Langevin equation, with the aid of the convolution theorem, has a convenient result in the search for admittance.

$$\left(-i\omega m^* + \zeta(\omega) - \frac{k}{i\omega}\right)\hat{v}(\omega) = \hat{E}(\omega) \tag{5.7}$$

$$\mathcal{Y}(\omega) = \frac{1}{-i\omega m^* + \zeta(\omega) - k/i\omega} \tag{5.8}$$

Where m^* is the effective mass of the particle and ζ is friction. The effective mass of the particle is determined by the mass of the particle m_p as well as the mass of the fluid displaced by the particle m_f, which itself is determined by the radius of the particle a and the density of the fluid ρ_f. The friction is determined by the radius of the particle, the density of the fluid, and the FDDV.

$$m^* = m_p + \frac{1}{2}m_f, \quad m_f = \frac{4}{3}\pi a^3 \rho_f \tag{5.9}$$

$$\zeta(\omega) = 6\pi\eta(\omega)a\big[1 + \beta(\omega)a\big], \quad \beta(\omega) = \sqrt{\frac{-i\omega\rho}{\eta(\omega)}} \tag{5.10}$$

For purposes computation, it is easiest to normalize several functions involved in the derivation, including the FDDV and the VACF. These normalized, or *reduced* functions will be hereafter referred to as RFDDV $\hat{G}_v(\omega)$ and RVACF $\hat{F}(\omega)$ respectively.

$$\eta(\omega) = \eta_0 \hat{G}_v(\omega) \tag{5.11}$$

$$\hat{C}(\omega) = \frac{k_B T}{m^*}\hat{F}(\omega) \tag{5.12}$$

It is also convenient to introduce several timescale constants to reduce complication of the following formulae.

$$\tau_m = \frac{m^*}{6\pi\eta_0 a} \tag{5.13}$$

$$\tau_k = \frac{6\pi\eta_0 a}{k} \tag{5.14}$$

$$\tau_v = \frac{a^2\rho_f}{\eta_0} \tag{5.15}$$

Using Equation 5.5, it is possible to restate the results of the Fluctuation Dissipation theorem in terms of the reduced functions.

$$\hat{F}(\omega) = m^* \mathcal{Y}(\omega) \tag{5.16}$$

The results for the admittance may be expanded, as well as the results for friction. The combination will be the source of the relation between the RFDDV and the RVACF. The function Γ will be created for analytical convenience.

$$\frac{\zeta(\omega)}{6\pi\eta_0 a} = \frac{\tau_M}{\hat{F}(\omega)} + i\omega\tau_M + \frac{1}{i\omega\tau_k} \tag{5.17}$$

$$\Gamma = \frac{\tau_M}{\hat{F}(\omega)} + i\omega\tau_M + \frac{1}{i\omega\tau_k} \tag{5.18}$$

$$\hat{G}_v(\omega)\left[1 + \sqrt{\frac{-i\omega\tau_v}{\hat{G}_v(\omega)}}\right] = \Gamma \tag{5.19}$$

$$\hat{G}_v(\omega)^2 + \left(i\omega\tau_v - 2\Gamma\right)\hat{G}_v(\omega) + \Gamma^2 = 0 \tag{5.20}$$

The final steps in the derivation are purely algebraic, and the important result is given below [8].

$$\hat{G}_v(\omega) = \left[\sqrt{\frac{\tau_M}{\hat{F}(\omega)} + i\omega\left(\tau_M - \frac{1}{4}\tau_v\right) + \frac{1}{i\omega\tau_k}} - \frac{1}{2}\sqrt{-i\omega\tau_v}\right]^2 \tag{5.21}$$

5.2 Fluid Classification

The ability to analytically relate the time series of the brownian motion to the frequency-dependent dynamic viscosity means that the techniques of optical microrheology are sufficient to determine very fundamental aspects of fluid behavior. Using the above result, it is possible to detect which fluid model fits best to a given sample fluid.

Chapter 6

Analytical Methods

In order to access the utility of the method of determining the dynamic viscosity of a fluid given a time series of brownian motion illustrated by Equation 5.21, the computational viability of the analysis must be confirmed.

6.1 Direct Computation

The direct computation of the form given by Equation 5.21 involves three major steps. The first step takes the initial position data in the time domain and converts it into the velocity autocorrelation function in the time domain. The second step coverts the time-domain VACF to a frequency-domain VACF. Finally, the third step converts the VACF in the fourier domain to the frequency dependent dynamic viscosity FDDV.

$$\begin{aligned} x(t) &\rightarrow C(t) \\ C(t) &\rightarrow \hat{C}(\omega) \\ \hat{C}(\omega) &\rightarrow \eta(\omega) \end{aligned}$$

6.1.1 Time Domain VACF

Calculation of the time-domain VACF begins with initial data, which is a time series of voltage measurements. These voltage measurements cor-

respond to displacements, and after a quick rescaling, the full time series of position $x(t)$ is available. In order to reduce noise, the full time series of position is binned and smoothed with a flat window function, producing the binned time series of position $x_b(t)$. With a window of length k, the binned time series of position may be specifically defined.

$$x_b(t) = \frac{1}{k} \sum_{i=t-k}^{t} x(i) \tag{6.1}$$

It is worthy of noting that this method of binning data is *linear* binning, and there are many other methods by which data may be binned. For instance, in some analyses the window length k might vary with time index i. It is also possible to use non-uniform window functions, such as an exponential increasing with the index i or gaussian centered around the middle of the window. Overall, binning the data reduces noise by reducing local variability in the time series.

After the time series of position has been binned, the velocity $v(t)$ must be computed; however, unlike the rest of the analysis, the velocity may be computed directly without the introduction of much numerical error. The velocity may be computed in the expected way, as a scaled difference of the binned position time series.

$$v(t) = \frac{x_b(t) - x_b(t-1)}{\tau} \tag{6.2}$$

Once the time domain velocity has been calculated, the autocorrelation function of the velocity $C(t)$ must be computed. The direct method of computation

seems to be straight-forward as shown in Equation 6.3; however, there is non-trivial numerical error introduced due to the discretized approximation to the true Fourier relation. Thankfully, the Wiener-Khinchin Theorem relates the autocorrelation function $R_{xx}(t)$ of a variable $x(t)$ to its power spectral density $S_{xx}(\omega)$ (PSD), which provides an alternate, albeit indirect method of computation. In order to utilize this method of indirect computation, the PSD must be computed according to Equation 6.4, at which point the VACF may be computed according to Equation 6.5, or its corresponding numerical approximation Equation 6.6.

$$C(t) = \frac{1}{N-k} \sum_{t'=1}^{N-k} v(t')v(t'+t) \tag{6.3}$$

$$S_{vv}(\omega) = \frac{(\Delta t)^2}{\tau_{max}} \left| \sum_{t=1}^{N} v(t) e^{-i\omega t} \right|^2 \tag{6.4}$$

$$C(t) = \int_0^{\infty} S_{vv}(\omega) e^{i\omega t} d\omega \tag{6.5}$$

$$C(t) = \sum_{\omega=0}^{\Omega} S_{vv}(\omega) e^{i\omega t} \tag{6.6}$$

For more information about power spectral densities or the Wiener-Khinchin Theorem, see Appendices A.3 or A.4 respectively.

6.1.2 Frequency Domain VACF

Once the time domain VACF $C(t)$ has been computed, the Fourier transform of the VACF $\hat{C}(\omega)$ must be found. However, there are multiple sources of numerical error involved in this step which deserve special attention.

Though it will be discussed at length in the next section, it is sufficient for now to say that the Fourier transform of the VACF is found, and move on with the computation.

6.1.3 Frequency Dependent Dynamic Viscosity

Finally, the frequency dependent dynamic viscosity (FDDV) is computed according to Equation 5.3. This final stage in the computation is performed directly, and there is little error introduced here.

6.2 Numerical Error

Unfortunately, the method of direct computation is prone to significant numerical error. Most of the numerical error centers around step 2 of the analysis, in which the time-domain VACF is converted to a frequency-domain VACF. We have used several methods to reduce the numerical error in the analysis of step 2, most of which relate to complete Fourier techniques.

Ideally, the second step of analysis would be performed according to a general Fourier transform, represented in Equation 6.7. However, there are multiple sources of numerical error introduced by such a method. First, this is a discrete approximation to an integral, which introduces some unavoidable error. Second, due to experimental limitation, the observations take place during a finite time interval $I_{obs} = [t_1, t_2]$. The finite window of observation necessitates a split in the integral representation of the Fourier transform into three regions, as shown in Equation 6.8. Region I contains timescales shorter than

we could possible observe, Region II contains timescales actually observed, and Region III contains timescales too long for experimental observation.

$$\hat{C}(\omega) = \int_0^\infty C(t)e^{-i\omega t}dt \tag{6.7}$$

$$\hat{C}(\omega) = \hat{C}_I(\omega) + \hat{C}_{II}(\omega) + \hat{C}_{III}(\omega) \tag{6.8}$$

$$\hat{C}_I(\omega) = \int_0^{t_1} C(t)e^{-i\omega t}dt \tag{6.9}$$

$$\hat{C}_{II}(\omega) = \int_{t_1}^{t_2} C(t)e^{-i\omega t}dt \tag{6.10}$$

$$\hat{C}_{III}(\omega) = \int_{t_2}^\infty C(t)e^{-i\omega t}dt \tag{6.11}$$

6.2.1 Region I

In order to compute the VACF $C(t)$ for timescales to small to be observed, the values may be interpolated given the theoretical end behavior of $C(0) = 1$ due to perfect correlation of identical time series. There are several methods for interpolation; however, linear interpolation reduces the numerical error well enough, and can be adjusted to the form of Equation 6.12.

$$\hat{C}_I(\omega) = \left(\frac{\hat{C}(\omega_1) - 1}{\omega_1}\right)\omega \tag{6.12}$$

6.2.2 Region II

Since Region II was directly observed, the normal method of computation should be sufficient; however, the numerical error introduced by the

fast-fourier-transform (FFT) algorithm was larger than expected. In order to compensate for this error, the Filon Integration algorithm was used. The Filon algorithm has the advantage of greater accuracy over the FFT algorithm due to the quadratic expansion's higher degree of granularity than the linear expansion of the basis-fourier transform. Fundamentally, Euler's Identity is used to expand the conventional Fourier Transform into two parts, a complex part and an imaginary part, both of which become the integral of oscillatory functions, which is the necessary condition for use of the Filon Integration.

$$\hat{C}_{II}(\omega) = \int_{t_1}^{t_2} C(t)e^{-i\omega t}dt = \int_{t_1}^{t_2} C(t)\cos(\omega t)dt + i\int_{t_1}^{t_2} C(t)\sin(\omega t)dt \qquad (6.13)$$

The latter two terms in the end of Equation 6.13 can be computed with Filon numerical integration techniques, and well approximated according to the Filon formula. For more information on the Filon Integration technique, see Appendix B.2.

6.2.3 Region III

Fortunately, the long-timescale behavior of the Brownian motion is well approximated by a polynomial representation [8]. This behavior allows for the quick computation of missing tails, and serves to reduce the numerical error by a significant amount.

Chapter 7

Summary

In conclusion, Brownian motion can serve as a tool to determine microrheological properties of fluids and to help classify fluids according to known fluid models. Beginning with the framework of continuum mechanics, rheology studies the relationships between stresses and strains within physical materials. These materials may exhibit a variety of responses, including elastic, viscous, and viscoelastic responses. These responses are embodied in material models, of which fluid models are most relevant to the experiments in optical microrheology. The Maxwell fluid model is the most well understood fluid model, and Brownian motion trajectory statistics may be analytically determined for Maxwellian environments. Experimental observation of these Brownian trajectories allows for the computation of the frequency-dependent dynamic viscosity, which can help classify the fluid's characteristic properties. Such computation, though, it non trivial, and great analytical care must be taken to avoid numerical error. In the end, the result bears significant insight into the rheological classification of fluids, and signifies a step forward in the understanding of Non-Newtonian fluids.

Appendices

Appendix A

Mathematics

A.1 Autocorrelation Function

The autocorrelation function may be defined as a time lag expectation value, and is fundamentally used to detect non-randomness in data by determining the similarity between a signal and a time-lagged version of itself. When used with time-series data, the autocorrelation function is also used to detect memory effects.

$$R_{ff}(\tau) = \langle f(t)f(t-\tau)\rangle \tag{A.1}$$

For ergodic processes, the autocorrelation function may be described in terms of a time average.

$$R_{ff}(\tau) = \int_0^\infty f(t)f(t+\tau)dt \tag{A.2}$$

The autocorrelation function estimate may also be defined for discrete series, which is most useful in data analysis when signals are discretized.

$$\hat{R}_{ff}(\tau) = \frac{1}{(N-k)}\sum_{t=1}^{N-k} f(t)f(t+\tau) \tag{A.3}$$

A.2 White Noise

A white noise $\zeta(t)$ is defined as a stochastic variable whose properties do not vary with time, such that power spectral density is constant.

$$\frac{d}{d\omega}S_{\zeta\zeta}(\omega) = 0 \tag{A.4}$$

It is also worth noting that in the case of a Gaussian white noise, the following moments and autocorrelation function relations are known as well. Gaussian white noises are directly related to standard Wiener processes, and as such have direct meaning to Brownian motion.

$$\overline{\zeta(t)} = 0 \tag{A.5}$$

$$\langle \zeta(t)\zeta(t') \rangle = \delta(t - t') \tag{A.6}$$

A.3 Power Spectral Density

Power spectral density is a measure of continuous spectra that describes the distribution of power over a spectrum of a continuous variable $x(t)$.

$$S_{xx}(\omega) = \mathbb{E}\left[|\hat{x}(\omega)|^2\right] = \mathbb{E}\left[\int_0^\infty x^*(t)e^{i\omega t}dt \int_0^\infty x(t')e^{-i\omega t'}dt'\right] \tag{A.7}$$

A.4 Wiener-Khinchin Theorem

The Wiener-Khinchin theorem relates the power spectral density of a function in the frequency domain to the autocorrelation of the function in the time domain, and is very useful when computing the velocity autocorrelation function, since it allows for other-than-direct means of calculation.

$$S_{xx}(\omega) = \int_0^\infty R_{xx}(t) e^{-i\omega t} dt \tag{A.8}$$

$$R_{xx}(t) = \int_0^\infty S_{xx}(\omega) e^{i\omega t} d\omega \tag{A.9}$$

A.5 Convolution Theorem

The convolution theorem relates the convolution of two functions f and g with their Fourier transforms $\mathcal{F}\{f\}$ and $\mathcal{F}\{g\}$. Specifically, the Fourier transform of the convolution of two functions is equivalent to the product of the Fourier transforms of the two functions. This is useful when taking the Fourier transform of the general Langevin equation, since the frictional force is the result of the convolution of friction and particle velocity.

$$\mathcal{F}\{f * g\} = \mathcal{F}\{f\} \cdot \mathcal{F}\{g\} \tag{A.10}$$

Appendix B

Programming

B.1 Fast Fourier Transform (FFT)

The Fast Fourier Transform (FFT) is a computational algorithm to calculate the discrete Fourier Transform (DFT) of a given variable $x(t)$. The FFT is exact in the case of discrete data; however, the FFT will introduce some error when computing the DFT of a continuous variable, as a discrete approximation must be made.

$$x(k) = \sum_{i=0}^{N-1} x(i) e^{-i2\pi k \frac{i}{N}} \tag{B.1}$$

B.2 Filon Integration

The Filon integration algorithm is a technique to perform numerical integration that minimizes error by using a quadratic expansion approximation instead of a linear approximation for each panel of the segmentation. It is essentially a mapped Simpson's rule applied to the numerical integration [6].

$$\int_b^a f(x)\sin(kx)dx \approx h\left[Af(a)\cos(ka) - Af(b)\cos(kb) + BS_e + DS_o\right] \quad \text{(B.2)}$$

$$\int_b^a f(x)\cos(kx)dx \approx h\left[Af(a)\cos(ka) - Af(b)\cos(kb) + BC_e + DC_o\right] \quad \text{(B.3)}$$

$$A = \frac{1}{q} + \frac{\sin(2q)}{2q^2} - \frac{2\sin(q^2)}{q^3} \quad \text{(B.4)}$$

$$B = \frac{1}{q^2} + \frac{\cos^2(q)}{q^2} - \frac{\sin(2q)}{q^3} \quad \text{(B.5)}$$

$$D = \frac{4\sin(q)}{q^3} - \frac{4\cos(q)}{q^2} \quad \text{(B.6)}$$

Bibliography

[1] V. Balakrishnan. *Elements of Nonequilibrium Statistical Mechanics*. CRC Press, 2008.

[2] G. H. Batchelor. *An Introduction to Fluid Dynamics*. Cambridge University Press, 3 edition, 2000.

[3] Romesh C. Batra. *Elements of Continuum Mechanics*. American Institute of Aeronautics and Astronautics, 2006.

[4] Eugene C. Bingham. An investigation of the laws of plastic flow. *Bulletin of the Bureau of Standards*, 13:309–353, 1916.

[5] Eugene C. Bingham. *Fluidity and Plasticity*. McGraw-Hill Book Company, 1922.

[6] Stephen M. Chase and Lloyd D. Fosdick. An algorithm for filon quadrature. *Communications of the ACM*, 12(8):453–457, 1969.

[7] Pietro Cicuta and Athene M. Donald. Microrheology: a review of the method and applications. *Soft Matter*, 3:1449–1455, 2007.

[8] B. U. Felderhof. Estimating the viscoelastic moduli of complex fluids from observation of brownian motion of a particle confined to a harmonic trap. *Journal of Chemical Physics*, 134(20):204910, 2011.

[9] J. Ferguson and Z. Kembłowski. *Applied Fluid Rheology.* Elsevier Science Publishers LTD, 1991.

[10] Gerald G. Fuller. *Optical Rheometry of Complex Fluids.* Oxford University Press, New York, NY, 1995.

[11] M. L. Gardel, M. T. Valentine, D. A. Wietz, S. T. Wereley, and C. D. Meinhart. *Microrheology.* Springer-Verlag, 2005.

[12] A. Jeffrey Giacomin and Antony N. Beris. Letter to the editor: : Everything flows. *Journal of Rheology*, 59(2):473–474, 2015.

[13] Fancesco Del Giudice, Andrew Glidle, Francesco Greco, Paolo Antonio Netti, Pier Luca Maffettone, Jonathon M. Cooper, and Manlio Tassieri. Microrheology with optical tweezers: Measuring the solutions' relative vistcosity at a glance. *Cornell University Library*, 2014.

[14] G. R. Grimmett and D. R. Stirzaker. *Probability and Random Processes.* Oxford University Press, 2 edition, 1992.

[15] Stefan Hergarten. Basics of continuum mechanics: Elastic behaviour and poroelasticity.

[16] Fridtjov Irgens. *Rheology and Non-Newtonian Fluids.* Springer, 2014.

[17] Tongcang Li. *Ph.D.* PhD thesis, University of Texas at Austin, May 2011.

[18] Tongcang Li, Simon Kheifets, David Medellin, and Mark G. Raizen. Measurement of the instantaneous velocity of a brownian particle. *Science*, 328(5986):1673–1675, 2010.

[19] F. C. MacKintosh and C. F. Schmidt. Microrheology. *Current Opinion in Colloid & Interface Science*, 4:300–307, 1999.

[20] Robert M. Mazo. *Brownian Motion: Fluctuations, Dynamics, and Applications*. Number 112 in International Series of Monographs on Physics. Oxford University Press, 2008.

[21] Miles J. Padgett, Justin E. Molloy, and David McGloin, editors. *Optical Tweezers*, pages 1–34. Chapman and Hall/CRC, 2015/05/10 2010.

[22] Daniel V. Schroeder. *An Introduction to Thermal Physics*. Addison Wesley Longman, 2000.

Index